

ANALYSIS OF HOM PROPERTIES OF SUPERCONDUCTING PARALLEL-BAR DEFLECTING/CRABBING CAVITIES*

S.U. De Silva^{1,2#}, J.R. Delayen^{1,2},

¹Center for Accelerator Science, Old Dominion University, Norfolk, VA 23529, USA.

²Thomas Jefferson National Accelerator Facility, Newport News, VA 23606, USA.

Abstract

The superconducting parallel-bar cavity is currently being considered for a number of deflecting and crabbing applications due to improved properties and compact design geometries. The 499 MHz deflecting cavity proposed for the Jefferson Lab 12 GeV upgrade and the 400 MHz crab cavity for the proposed LHC luminosity upgrade are two of the major applications. For high current applications the higher order modes must be damped to acceptable levels to eliminate any beam instabilities. The frequencies and R/Q of the HOMs and mode separation are evaluated and compared for different parallel-bar cavity designs.

INTRODUCTION

In the proposed LHC luminosity upgrade the crab cavities will be used at two interaction points (IPs) in the LHC collider ring operating in a local crabbing scheme. At one of the interaction points the beam will be crabbed horizontally and in the other in vertical direction. One of the requirements in the cavity design is the dimensional constraint of 194 mm separation of the two parallel beam lines of 84 mm beam aperture diameter. This restricts the cavity diameter to be 300 mm or less. The crabbing system is required to deliver a peak transverse kick of 10 MV per beam at each side of the IP.

The 400 MHz superconducting parallel-bar cavity [1] proposed for LHC luminosity upgrade has been modified from the initial rectangular shaped geometry in to the cylindrical geometry as shown in Fig. 1, with improved electromagnetic and mechanical properties; to meet the design requirements.

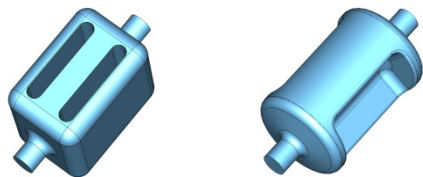


Figure 1: Rectangular shaped (left) and cylindrical shaped (right) parallel bar cavities.

The higher order modes (HOMs) in any cavity geometry may get activated when the harmonics of the beam current coincide with HOM frequencies of the

cavity. The wake fields generated with the activation of HOMs may act upon single or multiple bunches depending on the decay time of the HOMs. These effects may lead to beam instabilities and further into beam losses and can be minimized to an acceptable level by damping using couplers and filters.

The study HOM properties are equally important as the cavity properties in applications like LHC with higher average beam current (~500 mA). In this paper different geometries of the 400 MHz parallel-bar cavities are analyzed to determine the evaluation of modes, mode separation and corresponding R/Q values for the modes.

PARALLEL-BAR DESIGN GEOMETRY

Parallel-bar geometries with a cylindrical outer wall are analyzed for different orientations of bar shapes as shown in Fig. 2.

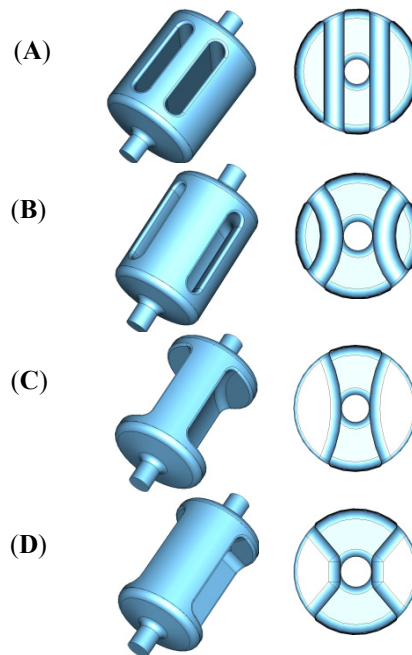


Figure 2: Cylindrical shaped parallel-bar geometries (left) with (A) straight bars (B) curved bars (C) bars merged to the side walls and (D) trapezoidal bars with the corresponding vertical cross sections (right).

The designs are compared to determine a compact design with improved properties such as lower and balanced peak surface fields, higher shunt impedance, and mechanical stability. The properties of each design are listed in Table 1.

*Authored by Jefferson Science Associates, LLC under U.S. DOE Contract No. DE-AC05-06OR23177. The U.S. Government retains a non-exclusive, paid-up, irrevocable, world-wide license to publish or reproduce this manuscript for U.S. Government purposes.

Part of this work was done in collaboration with and supported by Niowave Inc. under the DOE STTR program.

#sdesilva@jlab.org

Table 1: Properties of the parallel-bar structures of rectangular shaped design and cylindrical shaped designs with straight bars, curved bars, with bars merged on to the walls and trapezoidal bars

Parameter	Rectangular Design (Fig. 1)	Cylindrical Designs				Units
		Straight Bars (Fig.2 (A))	Curved Bars (Fig.2 (B))	Bars merged onto side walls (Fig.2 (C))	Trapezoidal Bars (Fig.2 (D))	
Frequency of π mode	400.0	400.0	400.0	400.0	400.0	MHz
$\lambda/2$ of π mode	375.0	375.0	375.0	375.0	375.0	mm
Frequency of 0 mode	411.0	492.6	650.95	673.28	729.5	MHz
Frequency of near neighbour mode	411.0	492.6	581.53	585.42	593.4	MHz
Cavity length	444.7	520.0	520.0	520.0	520.0	mm
Cavity diameter / width	300.0	406.8	356.0	375.3	339.8	mm
Cavity height	383.2	-	-	-	-	mm
Bars width at waist	55.0	65.0	65.0	-	-	mm
Bars length	330.0	345.0	345.0	345.0	345.0	mm
Bars height / curved height	383.2	398.0	324.0	350.0	80.0	
Aperture diameter	84.0	84.0	84.0	84.0	84.0	mm
Deflecting voltage (V_T^*)	0.375	0.375	0.375	0.375	0.375	MV
Peak electric field (E_P^*)	2.2	2.67	3.27	3.25	3.82	MV/m
Peak magnetic field (B_P^*)	7.9	7.89	7.83	7.99	7.09	mT
B_P^* / E_P^*	3.6	3.0	2.39	2.46	1.86	mT/(MV/m)
Energy content (U^*)	0.14	0.14	0.17	0.2	0.19	J
Geometrical factor	74.1	92.7	112.0	112.1	119.7	Ω
$[R/Q]_T$	413.3	388.7	321.2	281.8	312.2	Ω
$R_T R_S$	3.1×10^4	3.6×10^4	3.6×10^4	3.2×10^4	3.7×10^4	Ω^2

At $E_T^* = 1$ MV/m

In the parallel-bar design the main contribution for the deflection is from the transverse electric field between the parallel bars, where the magnetic field is between the bars connecting the outer wall generating high surface fields in those areas. The parallel-bar designs are optimized to achieve low surface field ratios and higher shunt impedance. The geometries with cylindrical outer conductors have similar properties in peak surface electric (E_P) and magnetic (B_P) fields, however the designs with curved parallel bars tends to have higher peak surface electric fields compared to other designs.

The advantage of cylindrical shaped design with trapezoidal bars is the ability to reduce surface magnetic fields with wider bars connecting to the outer wall. Furthermore the straight sections of inner bar height create a uniform transverse electric field across the beam aperture. The shapes of the bars are optimized specifically to lower the peak surface magnetic field with an increase in the peak surface electric field. The design is optimized for tolerable peak surface fields of $E_P=35$ MV/m and $B_P=65$ mT with a field balancing ratio of $B_P/E_P=1.86$ mT/(MV/m). The final achievable transverse voltage per cavity is shown in Table 2, where the design requirement can be achieved with 3 parallel-bar crabbing cavities.

Table 2: Achievable transverse voltage (V_T)

E_P/E_T	B_P/E_T (mT/(MV/m))	E_P at $V_T = 3$ MV	B_P at $V_T = 3$ MV
3.82	7.09	35 MV/m	65 mT

The design with the trapezoidal bars has the highest geometrical factor and $R_T R_S$ (R_T – Transverse shunt impedance, R_S – Surface resistance), reducing the power dissipation through the walls. Also this design has the smallest diameter compared to other designs. The rectangular shaped designs with larger flat surfaces are more susceptible to mechanical deformations due to liquid helium pressure and pressure due to electromagnetic fields. In contrast the cylindrical shaped design will experience low mechanical deformations and moreover the curved bars connecting the outer conductor gives added support to rigidity. The end plates with a slope also make the design more robust and can be used for easy removal of material during chemical processing and cleaning.

HIGHER ORDER MODE PROPERTIES

The fundamental deflecting mode has the lowest frequency in the parallel-bar geometry. The HOMs in these geometries cannot be categorized as monopole modes, dipole modes and so on as in conventional cavities. The modes are categorized as shown in Table 3.

Table 3: Types of HOMs in parallel-bar cavity

Field on axis	Type of Mode
E_x, H_y	Deflecting in horizontal direction
E_z	Accelerating
E_y, H_x	Deflecting in vertical direction
H_z	Does not couple to the beam

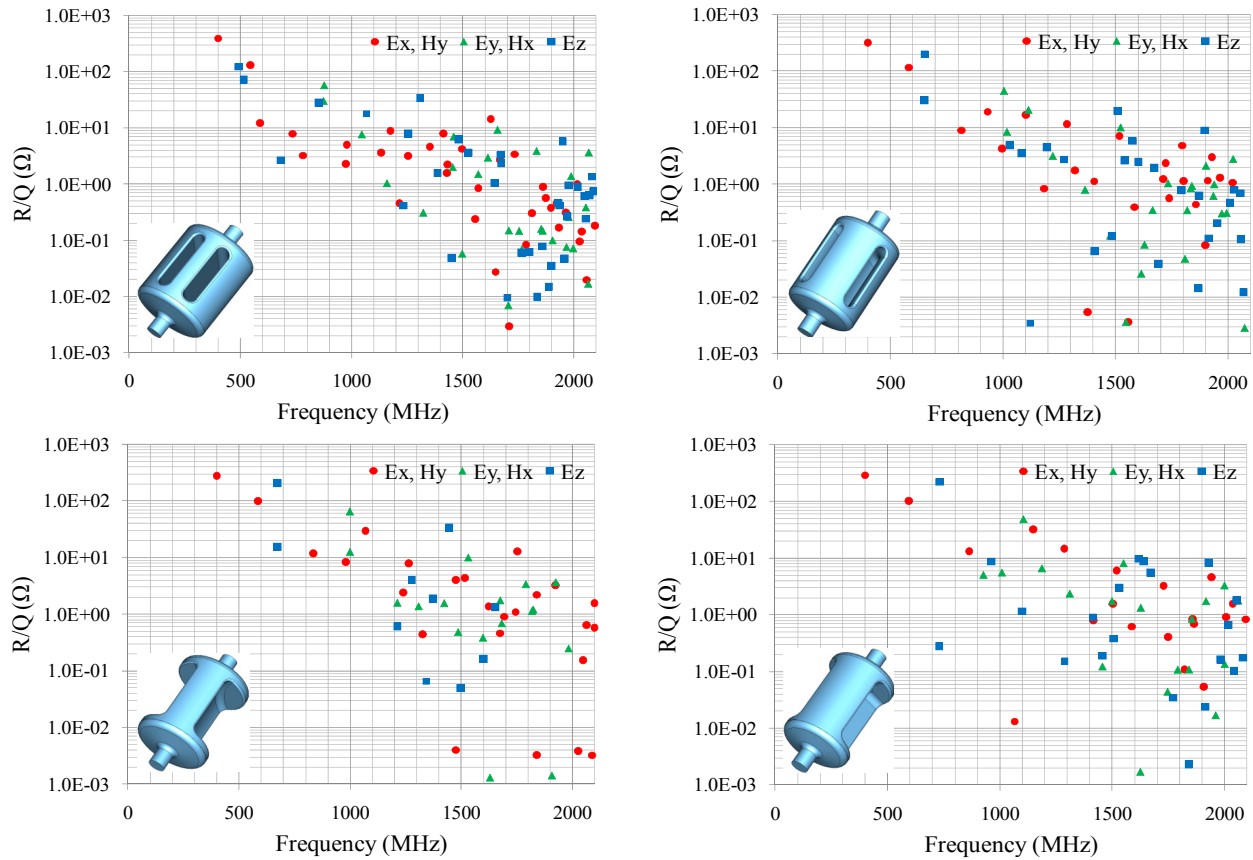


Figure 3: R/Q values for cylindrical shaped parallel-bar geometries with straight bars (top left), curved bars (top right), bars merge on to the side walls (bottom left) and trapezoidal bars (bottom right).

The R/Q values are calculated up to 2.1 GHz, which is the lowest beam aperture cut off frequency of TE_{11} mode given by $f_c = J'_1 c / 2\pi R$ where $J'_1 = 1.84$ is the first zero of the Bessel function J'_1 , c is the speed of light and $R = 42$ mm is the beam aperture radius. The modes above the cut off frequency pass through the beam aperture. The R/Q values are calculated by evaluating the field on axis for all the modes in each of the parallel-bar geometry as shown in Fig. 3, using the methods specified in [2]. For the modes with transverse field the R/Q values are also calculated and compared using the Panofsky Wenzel Theorem [3, 4] with better than 1% agreement.

The fundamental mode has the highest R/Q in the parallel-bar geometry. The designs with straight and curved bars have a higher number of low-frequency modes compared to other designs. Merging the outer bar wall into the outer conductor of the cavity eliminates the modes trapped in that area, hence reducing the number of modes and also widens the modes separation. The wider mode separation and fewer modes make the parallel-bar cavity with the trapezoidal bars attractive in damping the HOMs.

The cylindrical shaped designs with the curved loading elements have a mode separation of at least 180 MHz between the fundamental mode and the next neighbor mode as shown in Table 2. This makes the damping of the next neighbor mode easier preventing mixing of modes.

CONCLUSION

The cavity properties and HOM properties are analyzed for four different cylindrical shaped parallel-bar geometries. This cavity geometry has no Lower Order Modes. The attractive features in the design with trapezoidal bars are the balanced peak surface fields and higher shunt impedance. The cavity properties meet the transverse voltage requirement of the LHC crab cavity with 3 cavities per beam. The fewer modes and wider mode separation also makes the parallel-bar cavity very attractive in HOM damping.

ACKNOWLEDGEMENTS

We want to thank Celine Brughera for her help with the design optimization and mode properties calculations.

REFERENCES

- [1] J.R. Delayen and H. Wang, Phys. Rev. ST Accel. Beams 12, 062002 (2009).
- [2] S.U. De Silva and J.R. Delayen, Proceedings of IPAC'10, Kyoto, Japan, p. 3075 (2010).
- [3] W.K.H. Panofsky and W.A. Wenzel, Rev. Sci. Instrum. 27, 967 (1956).
- [4] M.J. Browman, "Using the Panofsky-Wenzel Theorem in the Analysis of Radio-Frequency Deflectors", Proceedings of PAC'93, Washington, p. 800 (1993).